Review Paper

MODELING TISSUE HEATING FROM EXPOSURE TO RADIOFREQUENCY ENERGY AND RELEVANCE OF TISSUE HEATING TO EXPOSURE LIMITS: HEATING FACTOR

Kenneth R. Foster,[1] Marvin C. Ziskin,[2] Quirino Balzano,[3] and Giorgi Bit-Babik[4]

Abstract—**This review/commentary addresses recent thermal and electromagnetic modeling studies that use image-based anthropomorphic human models to establish the local absorption of radiofrequency energy and the resulting increase in temperature in the body. The frequency range of present interest is from 100 MHz through the transition frequency (where the basic restrictions in exposure guidelines change from specific absorption rate to incident power density, which occurs at 3–10 GHz depending on the guideline). Several detailed thermal modeling studies are reviewed to compare a recently introduced dosimetric quantity, the heating factor, across different exposure conditions as related to the peak temperature rise in tissue that would be permitted by limits for local body exposure. The present review suggests that the heating factor is a robust quantity that is useful for normalizing exposures across different simulation models. Limitations include lack of information about the location in the body where peak absorption and peak temperature increases occur in each exposure scenario, which are needed for careful assessment of potential hazards. To the limited extent that comparisons are possible, the thermal model (which is based on Pennes' bioheat equation) agrees reasonably well with experimental data, notwithstanding the lack of theoretical rigor of the model and uncertainties in the model parameters. In particular, the blood flow parameter is both variable with physiological condition and largely determines the steady state temperature rise. We suggest an approach to define exposure limits above and below the transition frequency (the frequency at which the basic restriction changes from specific absorption rate to incident power density) to provide consistent levels of protection against thermal hazards. More research is needed to better validate the model and to improve thermal dosimetry in general. While modeling studies have considered the effects of variation in thickness of tissue layers, the effects of normal physiological variation in tissue blood flow have been relatively unexplored.**
Health Phys. 115(2):295–307; 2018

Key words: exposure; radiofrequency; radiation; nonionizing; radiofrequency; safety standards

INTRODUCTION

MAJOR INTERNATIONAL exposure guidelines for radiofrequency (RF) energy (nominally, 3 kHz–300 GHz) have been in place for many years. These include Institute of Electrical and Electronics Engineers (IEEE) C95.1-2005 and C95.1a-2010 (collectively referred to as IEEE standards; IEEE 2005/2010) and the limits of the International Commission on Non-Ionizing Radiation Protection (referred to as ICNIRP guidelines; ICNIRP 1998 and 2009). These limits, together with those enforced by the U.S. Federal Communications Commission (FCC 1997), are all presently undergoing revision and updating. This present contribution is third in a series of reviews/commentaries on RF exposure limits as related to thermal hazards (Foster et al. 2016, 2017).

Since the early 2000s, a series of increasingly detailed studies have examined the absorption of RF energy in the body from external sources using numerically segmented models of the body derived from magnetic resonance imaging (MRI) or computed tomography (CT) images. A number of these studies have estimated the resulting temperature increase in tissue, in most cases using thermal models based on Pennes' bioheat transfer equation (BHTE) (Pennes 1948).

There has been a corresponding increase in emphasis on the use of thermal models to develop and refine exposure limits. Bakker et al. (2011) proposed to "defin[e] limits on [localized peak temperature increase] for specified durations of exposure." In a later presentation, ICNIRP Chair van Rongen (2016) considered setting an "operational threshold based on exposure-effect relation" rather than on an experimentally determined "health effect threshold." As related to thermal hazards, this implies the use of thermal models to supplement direct experimental data related to thermal hazards.

For background, the IEEE standards and ICNIRP guidelines have two sets of limits. Basic restrictions (BRs),

[1]Department of Bioengineering, University of Pennsylvania, 240 Skirkanich Hall, 210 S. 33rd Street, Philadelphia, PA 19104; [2]Temple University Medical School, 3420 N. Broad Street, Philadelphia, PA 19140; [3]Department of Electrical and Computer Engineering, University of Maryland, College Park MD 20742; [4]Chief Technology Office, Motorola Solutions, Inc., Fort Lauderdale, FL 33322.

G.B.-B. is an employee of Motorola Solutions, a company that might be affected by revision of exposure limits; all other authors declare no conflict of interest.

For correspondence contact: Kenneth R. Foster, Department of Bioengineering, University of Pennsylvania, 240 Skirkanich Hall, 210 S. 33rd Street, Philadelphia, PA 19104, or email at **kfoster@seas.upenn.edu**.

(*Manuscript accepted* 16 *January* 2018)
0017-9078/18/0

DOI: 10.1097/HP.0000000000000854

expressed in terms of field strength or absorbed power level within the body, are intended to be the biologically relevant measure of exposure. Reference levels are secondary limits, expressed in terms of field strengths outside the body, and are intended to be directly measurable quantities that, if respected, will ensure compliance with the BRs. All three limits (FCC, ICNIRP, and IEEE) have separate provisions for public and occupational exposures. (Terminologies vary but all three sets of limits draw equivalent distinctions. FCC does not distinguish between basic restrictions and reference levels but provides the equivalent of BRs in its limits for portable devices that are used within 20 cm of the body. Also, the IEEE calls its limits a "standard" while ICNIRP and FCC use the term "guidelines.")

The BRs in the three limits are summarized in Table 1. For whole-body exposure, the BR is expressed as the specific absorption rate or SAR (W kg^{-1}) averaged over the entire body mass and is intended to limit the total thermal load imposed on the body. The BR for local exposure is expressed as the peak SAR value within the body averaged over a specific mass of tissue (the peak spatial SAR or psSAR) and is principally intended to limit local temperature increase. Above 3–10 GHz (depending on the guideline), both ICNIRP and IEEE change their BRs from limits expressed as SAR to limits expressed as incident power density due to the decline in energy-penetration depth with increasing frequency and corresponding difficulty in measuring SAR.

To avoid misunderstanding, the following discussion pertains to thermal hazards only. The committees drafting the limits evaluated reports of low-level or nonthermal (not thermally produced) effects and concluded that, with few exceptions, the only proven hazards of RF exposure in the presently considered frequency range are associated with excessive tissue heating. The scientific literature, which includes many reports of nonthermal effects, is periodically re-evaluated as the limits are updated, and the understanding of potential hazards of RF exposure is always subject to revision as more data become available.

The present review focuses on the relation between the psSAR and the resulting peak increase in tissue temperature given in terms of the heating factor H.

Thermal models and heating factor

Pennes' BHTE can be written in simplified form as

$$k\nabla^2 T - \rho^2 C m_b T + \rho SAR = \rho C \frac{dT}{dt}, \qquad (1)$$

where T is the temperature increase (°C) above the baseline (pre-exposure) level (other parameters are defined in Table 2). Eqn (1) is subjected to convective boundary condition at the tissue-air interface

$$k\frac{\partial T}{\partial n} = -h(T_{sur} - T_{air}), \qquad (2)$$

where T_{sur} and T_{air} are the surface temperatures of the tissue and surrounding air and h is a heat transfer coefficient, which is typically chosen to be in the range of 5–10 W m^{-2} $^{o}C^{-1}$ for ordinary room environmental conditions.

The SAR at any point in the tissue is defined as

$$SAR = \frac{\sigma E^2}{\rho}, \qquad (3)$$

where σ is the electrical conductivity (S m^{-1}) and E is the root-mean-square (RMS) electric field strength at that point (V m^{-1}).

Table 1. Basic restrictions in ICNIRP (1998), IEEE C95.1-2005 (2010), and FCC (1997) for local and whole-body exposures.[a]

Standard or guideline	ICNIRP (1998) 100 kHz –10 GHz	IEEE C95.1-2005 (2010) 100 kHz – 3 GHz	FCC (1997)
SAR limit for local exposure (psSAR, W kg^{-1})	General public: 2 (head, trunk) 4 (limbs)	Unrestricted (equivalent to general public): 2 (unspecified part of body) 4 (extremities and pinnae)	General public: 1.6 (unspecified body part) 4 (hands, wrists, feet, ankles, pinnae)
Averaging mass (g)	Occupational: 10 (head and trunk), 20 (limbs)	Restricted (equivalent to occupational): 10 (unspecified part of body) 20 (extremities and pinnae)	Occupational: 8 (unspecified body part) 20 (hands, wrists, feet, ankles, pinnae)
	Averaged over 10 g of contiguous tissue	Averaged over 10 g of tissue in shape of cube	Averaged over 1 g of tissue in shape of cube
	Also has a limit for specific absorption (total absorbed energy) for pulsed exposure mJ kg^{-1} (0.3–10 GHz)		
SAR limit for whole body exposure (W kg^{-1})	General public: 0.08 Occupational: 0.4 Averaged over whole body	General public: 0.08 Restricted (equivalent to occupational): 0.4 Averaged over whole body	General public: 0.08 Occupational: 0.4 Averaged over whole body

[a]Frequency range in which the basic restriction is defined in terms of absorbed power density (SAR).

Table 2. Definition of parameters in eqn (1) and values assumed for baseline model.[a]

k	Thermal conductivity	0.37 W m^{-1} °C^{-1}
C	Specific heat capacity	3,390 W s kg^{-1} °C^{-1}
ρ	Tissue density	1,109 kg m^{-3}
m_b	Tissue blood perfusion	1.8×10^{-6} m^3 kg^{-1} s^{-1} 10.8 mL (min 100 g)$^{-1}$ in units typically used in the physiology literature

[a] Thermal parameters for dry skin (from Hasgall et al. 2017).

A dimensional analysis of eqn (1) yields two time scales (τ_1, τ_2) that can be identified with heat transport by thermal convection by blood perfusion and thermal conduction, respectively:

$$\begin{aligned} \tau_1 &= 1/m_b\rho \approx 500 \text{ s} \\ \tau_2 &= L^2/\alpha \end{aligned} \quad (4 \text{ a, b})$$

where $\alpha = k\,(\rho C)^{-1}$ is the thermal diffusivity (9.8×10^{-8} m^2 s^{-1}) and L is the depth at which the local SAR has decreased to e^{-1} from its level at the surface (equal to one-half of the field penetration depth). The first of these (τ_1) characterizes the time scale for convective heat clearance due to blood perfusion, while the second (τ_2) characterizes the time scale for heat diffusion over distances comparable to the energy-penetration depth L. There are two corresponding distance scales (R_1, R_2):

$$\begin{aligned} R_1 &= \frac{\sqrt{k}}{\rho\sqrt{m_b c}} \approx 7 \text{ mm} \\ R_2 &= \sqrt{4\alpha t} \approx 0.5\sqrt{t} \text{ mm} \end{aligned} \quad (5 \text{ a, b})$$

The first of these (R_1) is a measure of the distance over which increases in local temperature are removed by effects of blood perfusion, and R_2 is the mean square distance over which heat diffuses in time t.

For a plane wave of RF energy incident on a planar half-space of homogeneous lossy material, the source term in eqn (1) is

$$\begin{aligned} SAR &= \frac{I_o T_{tr}}{\rho L} e^{-z/L} \\ &= SAR_o e^{-z/L} \end{aligned} \quad (6)$$

where I_o is the incident power density on the tissue (W m^{-2}) and T_{tr} is the energy transmission coefficient into the half-space. Table 1 in Foster et al. (2016) shows these quantities as functions of frequency for the parameter values in eqn (1). Above 10 GHz, the energy-penetration depth in tissue is 1–2 mm or less, and the thermal response of tissue to RF exposure is closely approximated by a model assuming purely surface heating (Foster et al. 2017).

It is useful to define the heating factor H as the ratio of the peak steady state increase in tissue temperature (ΔT) to the peak mass-averaged SAR in the body (psSAR) (Wainright 2007):

$$H = \frac{\Delta T_{max}}{psSAR} \left(^\circ\text{C kg W}^{-1}\right). \quad (7)$$

H depends on the size and shape of the averaging volume for the SAR and is influenced by the details of heat transfer in the region of highest SAR. In the discussion below, psSAR (10 g cube) is the mass-averaged SAR over a cubic volume of a 10 g mass.

Baseline model

For an insulated half-space (i.e., adiabatic boundary condition with $h = 0$), the steady state increase in surface temperature (T_{ss}) can be written as the product of the SAR at the surface (SAR_o) and an effective time constant τ_{eff} (Foster et al. 1998):

$$\begin{aligned} &T_{ss} = \frac{SAR_o}{C}\tau_{eff} \quad \text{(surface temperature, steady state)} \\ &\text{where} \\ &\tau_{eff} = \frac{\tau_2 - \sqrt{\tau_1\tau_2}}{\tau_2/\tau_1 - 1} \end{aligned} \quad (8 \text{ a, b})$$

The limiting values of T_{ss} are

$$\begin{aligned} T_{ss} &\rightarrow \frac{I_o T_{tr}}{LCm_b\rho^2} \quad \tau_2 >> \tau_1 \text{ (low frequency limit)} \\ &\rightarrow \frac{I_o T_{tr}}{\rho\sqrt{Cm_b k}} \quad \tau_1 >> \tau_2 \text{ (high frequency limit)} \end{aligned} \quad (9 \text{ a, b})$$

The transition between these limiting cases occurs at about 3 GHz for soft tissue (Fig. 2 in Foster et al. 2016).

The mass-averaged psSAR in a shell of thickness d immediately beneath the surface is

$$psSAR_d = \frac{SAR_o}{d} L\left(1 - e^{-d/L}\right), \quad (10)$$

leading to the heating factor H

$$\begin{aligned} &H = \frac{\tau_{eff} d}{CL(1 - e^{-d/L})} \\ &\text{For } d << L \text{ this approaches} \\ &H = \frac{1}{Cm_b\rho} = 0.15\,^\circ\text{C kg W}^{-1} \end{aligned} \quad (11 \text{ a, b})$$

The low-frequency limit, eqn (11b), can be obtained directly from the steady state solution to the BHTE for cases where thermal conduction is negligible compared to convection by blood flow, which is more likely to apply at low frequencies with large L.

The Green's function solution to the BHTE (Yeung and Atalar 2001) establishes a relation between the local SAR and the local temperature rise. If the heating pattern is radially symmetric and the effects of boundary conditions are ignored, the Green's function for the steady state solution to eqn (1) is

Table 3. Heating factors, baseline model.[a]

Frequency, GHz	L (cm): Energy penetration depth	T_{tr}: Energy transmission coefficient	τ_{eff} (s)	I_oT_{tr}: Absorbed power density at surface to result in T_{ss} = 1 °C, Wm^{-2}	H, based on 1 g psSAR °C kg W^{-1}	H, based on 10 g psSAR °C kg W^{-1}	Time required to reach 90% of T_{ss}(s)
0.1	5.2	0.29	447	439	0.145	0.161	1,100
0.3	3.1	0.38	414	282	0.143	0.169	1,000
1	1.9	0.45	372	195	0.141	0.182	970
3	0.9	0.47	290	122	0.139	0.218	850
10	0.19	0.49	108	66	0.168	0.36	700

[a]Calculated from Foster et al. (2016, 2017) using parameters in Table 2 of present paper.

$$G(r) = \frac{\rho}{4\pi kr} e^{-r/R_1}, \qquad (12)$$

where r is the radial distance from the observation point to a point source of heat. Apart from a constant factor, the steady state temperature increase at point r is the convolution of the Green's function with the SAR pattern. The BHTE has no provision for long-range convective transfer of heat by blood flow in major vessels; the local temperature increase is determined by the SAR pattern close to the measurement point with perhaps some contribution from heat conducted from nearby regions of tissue.

Table 3 summarizes the results of the baseline model using thermal parameters in Table 2 and electrical properties given by Foster et al. (2016, 2017). The heating factors were calculated using eqn (11), and thermal response times were calculated using a finite element program. The heating factor increases slowly with frequency above 1 GHz as L progressively decreases.

Anatomically detailed models

Over the past decade, several groups have evaluated RF exposure and temperature increase in anatomically detailed tissue models, in most cases considering numerous alternative-exposure scenarios (Table 4). The table also summarizes the values of the blood perfusion parameter m_b used in the studies, which is the parameter in the BHTE with the largest variability. Unless stated otherwise, in the following discussion H will be defined in terms of a volume-averaged SAR over 10 g of tissue in the shape of a cube (as used in the IEEE standard).

Planar models. Anderson et al. (2010) determined the SAR distribution and temperature increase in multilayer planar models subject to plane-wave exposure to RF energy. The investigators chose the thickness and thermal properties of the layers (representing skin, fat, and muscle) from a review of anatomical data, and they conducted a Monte Carlo analysis using a total of 32,000 different combinations of parameters (400 sets for each of eight body sites for 10 frequencies between 1–10 GHz). Table 5 summarizes the results of this analysis. Averaged over many simulations, a mean incident power density of 170 W m^{-2} or more (far above IEEE and ICNIRP reference levels) was needed at each frequency to produce a peak temperature increase of 1 °C, and heating factors were similar to those in the baseline (homogeneous) model (Table 5). Depending on frequency, the ratio of the 95th to 5th percentile temperature increases at the surface varied between 2 and 4.1 (Table 5). Consequently, for some combinations of parameters, the increase in surface temperature could be about twice as high as the average increase over the many simulations.

Heating factor in three-dimensional image-based models

Three groups have conducted detailed assessments of psSAR and temperature increases in image-based models of the head or whole body with overall similar results.

Head model

Hirata and Shiozawa (2003) were first to report a systematic analysis of the psSAR and peak temperature increase in image-based models of the head. These investigators considered a total of 660 different exposure scenarios involving RF exposure from dipoles located 1 cm away from the head and radiating 1 W (near-field exposure) at five frequencies between 0.9 and 2.45 GHz. The ears were either in a normal position or pressed against the head to simulate use of a mobile handset.

The peak temperature rise in the head and brain as well as psSAR (10 g cube) are summarized in Fig. 1 (from Hirata and Shiozawa 2003). The mean heating factor (the slope of the regression line in Fig. 1a) was 0.237 or 0.197 °C kg W^{-1} for unpressed or pressed ears. That paper did not state the location of the peak temperature increase in the brain, but a more recent paper by that group (Kodera et al. 2018), discussed below, indicates that the peak temperature rise in the brain occurs in the periphery of the brain close to the skull.

Whole-body model

Bit-Babik et al.[5] determined the SAR distribution and temperature increases in an image-based model of a human (Visible Man) exposed to plane-wave radiation incident from one of three directions, at either vertical or horizontal

[5]Bit-Babik G, Faraone A, Chou CK, Razmadze A, Zaridze R. Correlation between locally averaged SAR distribution and related temperature rise in human body exposed to RF field. BEMS 29th annual meeting, 11–15 June 2007, Kanazawa, Japan.

Table 4. Comparison of models used by studies reviewed here.

Study	Model used	Location of psSAR; location of peak temperature increase	Comment	Tissue blood perfusion (skin/fat/muscle)[a] 10^7 m^3 kg^{-1} s^{-1}
Baseline model (eqn1)	Homogeneous medium with thermal and electrical properties of dry skin	At surface	Results used for comparison with more detailed models.	18
Hirata and Shiozawa (2003)	Human head model, dipole antenna, 5 frequencies between 0.9 and 2.45 GHz, two polarizations, 18 feedpoints; "pressed" and "unpressed" ears	Near surface	Peak temperature increases in head and brain are 0.31 and 0.13 °C for FCC and 0.60 and 0.25 °C for ICNIRP limits (both limits for general public).	22/1.3/6.5
Bit-Babik et al.[b]	Whole-body exposure (Visible Man) 8 frequencies between 0.03–1 GHz),\ 3 directions of incidence and two polarizations	Close to or at surface, location on body or in the limbs, varies with frequency	All peak temperature increases below 1 °C (typically 0.1 °C) at reference level for the general public.	22/4.1/6.5
Anderson et al. (2010)	Multilayer plane model with layers representing human tissue of varying thickness and thermal properties. (1–10 GHz), plane-wave exposure	Close to or at surface	Monte Carlo analysis includes many combinations of thickness and properties of skin, fat layers based on anatomical data.	29/2.4/5.1
McIntosh et al. (2010)	Two head model (adult, 12 y old child); also partial-body model (upper legs and torso of adult model). Diverse sources including resonant dipoles at several locations near the head, and plane waves incident from different directions and with different polarizations. Calculations done at 1, 3, 6, 8, 10 GHz.	Both psSAR and T highest in superficial tissues (e.g., pinna, nose, eyelid) at all frequencies.	Exceptionally complete analysis in terms of exposure conditions. Peak temperature increases were located near the surface of body but their position varied with model and exposure condition.	29/2.4/5.1
Bakker et al. (2010, 2011)	Whole body models (2 adults, 6 children), 10–5,600 MHz), 12 different exposures using orthogonal plane waves; parameters varied	Location of peak temperature and psSAR "usually found at body protrusions." Median distance between locations of the peak temperature increase and 10 g psSAR ranged from 1.9–10.4 cm, and to the 1 g psSAR varied from 0.3 to 1.6 cm depending on the frequency.	Extensive sensitivity analysis (Monte Carlo). Recommends defining limits in terms of peak temperature increases over specified times.	16/4.5/4.7
Morimoto et al. (2016)	Head models including simplified (multilayer cubes) and image-based models; diverse exposure sources (dipoles) located 1.5 cm from head (1–30 GHz)	Both psSAR and peak T located close to surface of head near the ear.	Maximum psSAR in pinna and near surface of head.	22/1.3/6.5

[a]Converted to a consistent set of units assuming tissue density of 1,000 kg m^{-3}.

[b]Bit-Babik G, Faraone A, Chou CK, Razmadze A, Zaridze R. Correlation between locally averaged SAR distribution and related temperature rise in human body exposed to RF field. BEMS 29th annual meeting, 11–15 June 2007, Kanazawa, Japan.

polarization, at eight frequencies between 0.03 and 1 GHz. While not an original goal of the study, the work yielded values for psSAR and peak temperature rise in the body and consequently heating factors.

Fig. 2 summarizes results from Bit-Babik et al.[5] showing peak temperature increases produced by whole-body exposure to plane waves impinging on the body from several directions and polarizations at an incident power density of 10 W m^{-2} (the ICNIRP reference level for occupational exposures over much of the indicated frequency range). The peak temperature increases are generally less than 1 °C and occur at widely varying locations in the body from the extremities (leg or knee) at the lower frequencies to superficial tissues at various places in the body at the higher

Table 5. Incident power density for multilayer model required to produce a 1 °C increase in surface temperature (from Anderson et al. 2010).[a]

	Multilayer model (Anderson et al. 2010)			Baseline model	
f, GHz	Incident power density (plane waves) for 1 °C increase, W m^{-2} (mean over many simulations)	Ratio of 95th to 5th percentile power density for 1 °C increase of surface temperature.	Mean heating factor H, 10 g psSAR (°C kg W^{-1})	Incident power density to produce a 1 °C increase in surface temperature, W m^{-2}	Heating factor H, 10 g psSAR (°C kg W^{-1}) (eqn 11a)
1	267	4	0.27	430	0.18
2	170	2.7	0.28	320	0.20
3	184	3.4	0.29	259	0.22
4	212	4.1	0.29	216	0.25
5	225	3.9	0.30	191	0.27
6	225	3.2	0.30	172	0.30
7	217	2.6	0.31	158	0.32
8	204	2.4	0.31	149	0.34
9	192	2.2	0.32	141	0.35
10	181	2	0.33	136	0.37

[a]psSAR calculated for 10 g of tissue in the shape of a cube.

frequencies of the simulation. In some cases, the peak temperature increases occurred at points of contact between body surfaces (upper leg, where hand touches torso), which would vary greatly with body position. Except at the two lowest frequencies (30 and 70 MHz, which are close to the whole-body resonant frequency), the heating factor (slope of the regression line in Fig. 2) is 0.27 °C kg W^{-1}. Temperature increases at ICNIRP reference levels for the public would be a factor of five below those shown in Fig. 2. Over the frequency range of this study, the local temperature increases induced at the ICNIRP and IEEE reference levels (which apply to whole-body exposure) are modest and quite small for exposures at reference levels for the public.

Head and partial-body model

In an exceptionally complete analysis, McIntosh and Anderson (2010) calculated 1 g and 10 g psSARs (cubic averaging volumes) and peak temperature increases in image-based models of the heads of an adult and a 12-y-old child subject to RF exposure at 1, 3, 6, 8, and 10 GHz. The RF exposure was from transmitting antennas (half-wave dipoles) located 1 cm from the body and also from plane waves incident on the body from different directions and with different polarizations. The investigators also evaluated exposure to an image-based model of the torso and upper legs of an adult male. The results are summarized in Fig. 3, normalized to an incident power density of 10 W m^{-2}. The results show considerable scatter (perhaps because the results are

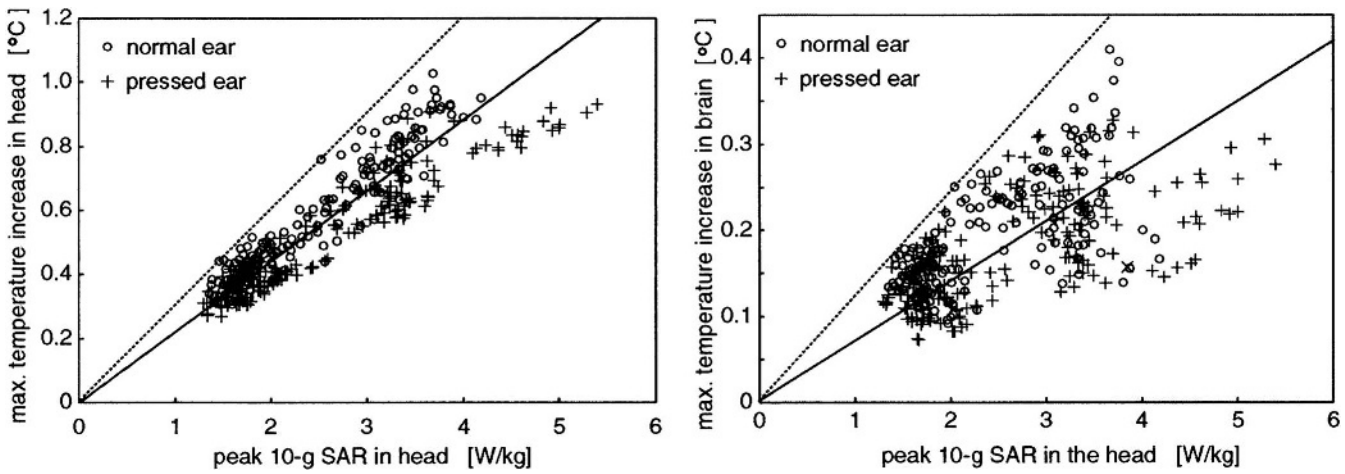

Fig. 1. Maximum temperature increase head and brain vs. psSAR (10 g over cubic volumes) in the head from RF exposure to dipole antennas located 1 cm from head. The figure shows results of a total of 660 simulations at different frequencies between 0.9 and 2.45 GHz and location of feed points. Two positions of the ear were considered, in a normal position and pressed against the surface of the head. Reprinted from Hirata and Shiozawa (2003) with permission of the authors and IEEE. Feed point input power was 1 W for all simulations. The regression line (solid) and the line indicating the maximum slope (dotted) are demonstrated.

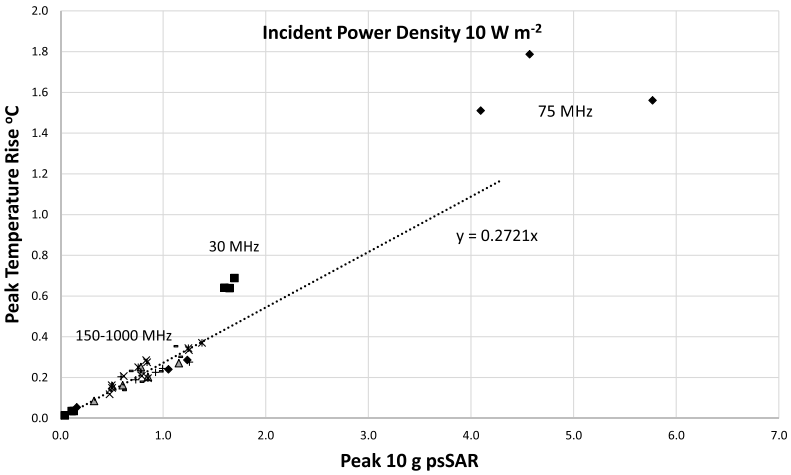

	■ 30	◆ 75	▲ 150	× 300	✳ 450	- 800	+ 1000	MHz
ICNIRP Limit	10	10	10	10	11	20	25	W m^{-2}
IEEE	10	10	10	10	15	27	33	W m^{-2}

Fig. 2. Maximum psSAR (average over 10 g cubic volume) and peak temperature increase in whole-body model exposed to plane-wave energy at an incident power density of 10 W m^{-2}, directed at the model from one of three incident directions and with vertical or horizontal polarization (based on Bit-Babik G, Faraone A, Chou CK, Razmadze A, Zaridze R: Correlation between locally averaged SAR distribution and related temperature rise in human body exposed to RF field. BEMS 29th annual meeting, 11–15 June 2007, Kanazawa, Japan). Regression line was calculated from results from 0.15–1 GHz and corresponds to a heating factor of approximately 0.27 °C kg W^{-1}. ICNIRP reference levels for occupational groups are also shown.

from both near-field and far-field exposures). The slope of the regression line (i.e., heating factor) is 0.24 °C kg W^{-1}, similar to that of other studies reviewed here. As in Bit-Babik et al.[5] the location of the peak temperature increases varied widely across the body but was generally located in superficial areas of the body (pinna, eyelid, sclera, upper lip, and skin at the base of the penis).

Whole-body models

Baker et al. (2011) modeled an entire "virtual family" including male and female adult and several child models. Fig. 6 from that study shows a false-color image of a child standing erect in a vertically polarized 2 GHz field. The image shows peaks in RF absorption in the finger of the model at 2.5 W kg^{-1} (10 g psSAR) at an incident power

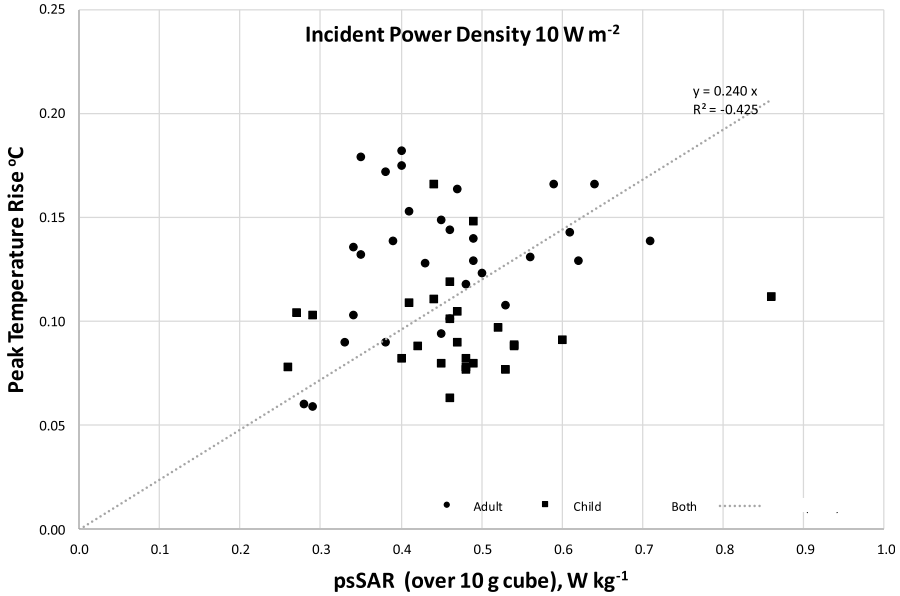

Fig. 3. Calculated peak temperature increases and 10 g psSAR (cubic volume) in adult and 12-y-old child model. Incident power density was 10 W m^{-2} (plane waves) and 10 W m^{-2} free-space power density averaged over 20 cm^2 area (dipoles). Figure drawn from Tables 2 and 3 in McIntosh and Anderson (2010).

level of 10 W m^{-2}. The peak temperature increase in the model was 0.66 °C, corresponding to a heating factor of 0.26 °C kg W^{-1}.

Head models

In an exceptionally complete set of simulations, Morimoto et al. (2016) studied RF absorption and thermal response in multiple image-based models subject to local exposure to the head from resonant dipoles located 1.5 cm from the models. The study determined heating factors for 14 frequencies of 1–30 GHz, evaluated using different algorithms to determine mass-averaged exposure. The results are presented at length by Morimoto et al. (2016). At 1 GHz the heating factor was 0.21 °C kg W^{-1} (10 g cubic averaging volume), increasing gradually to 0.38 °C kg W^{-1} at 10 GHz. The heating factors showed considerable variability and varied with different averaging algorithms, as discussed in detail by Morimoto et al. (2016).

Thermal response time. All of the thermal responses considered above are steady state temperature increases, which develop after several minutes of continuous exposure. Morimoto et al. (2017) evaluated the time-dependent response of simplified (multilayer cubes) and realistic (MRI-based) anatomical models of the head and trunk for several exposure scenarios (half-wave dipoles 1.5 cm from the model and plane-wave exposure) at several frequencies between 1 and 30 GHz. These investigators also modeled small-area exposures to millimeter waves (30 GHz) with beam diameters from 1 to 15 cm.

The thermal time constants, which the investigators defined as the time required to reach 63% of the final temperature increase, were in the range of roughly 200–400 s, which is consistent with 90% response times shown in Table 3. Shorter response times were found when the exposed area was smaller than about 4 cm in diameter, due to lateral diffusion of heat parallel to the skin surface. (For larger exposed areas, heat transfer was predominantly only in a direction normal to the surface of the tissue.) For further discussion see Foster et al. (2016).

Validity of thermal model. The validity of the BHTE has been debated since Pennes' original publication in 1948. The following discussion extends that in Foster et al. (2017) and Ziskin et al. (2018).

The validity of the BHTE is considered below with respect to internal and external validity.

Internal validity refers to the fundamental correctness of the formulation, in this case for heat transfer in tissue. In the BHTE, the blood perfusion term quantifies removal of heat from the tissue bed. In the conventional narrative concerning the BHTE, heat is removed from tissue by blood flow through the capillary bed. However, because of the high thermal diffusivity of tissue, capillaries are thermally equilibrated with the surrounding tissue and do not participate significantly in transport of heat from the tissue, which principally occurs at the level of thermally significant vessels of > 80–100 μm diameter (Baish 2014). In the physiology literature, "tissue blood perfusion" conventionally refers to delivery of blood to the capillary bed and is conceptually removed from the actual heat exchange processes that take place in tissue.

Nevertheless, there is a broad consensus that, while the BHTE is not an exact representation of heat transfer in tissue, it is a useful approximation to a decidedly very complex problem (Baish 2014). A more rigorous solution would require detailed consideration of vascular anatomy, which in most cases would be infeasible. However, the caveat is that the "blood perfusion" term in the BHTE "describes [the] collective thermal effect for tissue not adjacent to vessels which may introduce local convection" (Arkin et al. 1994), and the BHTE is prone to significant errors near thermally significant blood vessels (Arkin et al. 1994).

External validity refers to the ability of the model to predict experimental results that are independent of those used to derive the model parameters in the first place. Despite Pennes' paper having been cited more than 2,500 times since its publication, remarkably few authors have compared predictions of the BHTE against independently collected experimental data.

Walters et al. (2000) reported an extensive series of studies on thermal response in humans to exposure to millimeter waves. In those studies, 10 subjects were exposed on their backs to 3 s pulses of 94 GHz radiation at incident power densities up to 18,000 W m^{-2}. The exposure was sufficient to raise skin temperature from pre-exposure levels (approximately 34 °C, which is typical of skin temperature in ordinary room environments) to the threshold for thermal pain (43.9 °C) after each pulse. In those studies, eqn (1) accurately predicted the measured increases in skin temperature using off-the-shelf parameters similar to those in Table 1 with no further adjustment of parameters (Walters et al. 2000). However, the exposure conditions (short-term heating over small areas) were such that heat conduction was the dominant mode of heat flow. The thermal conductivity of tissue is determined chiefly by its bulk composition, chiefly water content, and varies little among soft tissues with similar water content.

By contrast, the blood flow parameter, which largely determines the steady state temperature increase, is subject to large intersubject and intrasubject variation. The value of m_b used by Morimoto et al. (2016) for cerebral blood flow was 50 mL (min 100 g)$^{-1}$ (in the mixed units used in the physiology literature). That is close to the mean of values [32–62 mL (min 100 g)$^{-1}$] reported for a group of 10 young male subjects under resting conditions (Hiura et al. 2014). Considerably lower and more variable cerebral blood flow values ranging 10–70 mL (min 100 g)$^{-1}$ were reported by

Foster-Dingley et al. (2015) in a group of 305 elderly individuals. Blood perfusion in the skin can vary by up to an order of magnitude, both in different parts of the body and with varying environmental temperatures (Hertzmann and Randall 1948; Johnson and Kellogg 2010). Consequently, there is considerable parameter uncertainty in the thermal models, which strongly affects calculations of steady state temperature increases.

Nevertheless, and rather surprisingly, the limited available data are in reasonable agreement with predictions of the BHTE using off-the-shelf parameters taken from compilations of data in the literature. Alekseev et al. (2005) measured temperature increases in the skin of subjects exposed to 42.25 GHz energy at an incident power density of 500 W m^{-2}. The steady state temperature increases (in the range of 3–4.5 °C) were consistent with predictions of eqn (1) using parameters in Table 1 (Foster et al. 2016). Alekseev et al. reported still better agreement by extending the BHTE to include a blood-flow-dependent "effective" thermal conductivity of tissue (Alekseev et al. 2005; Ziskin et al. 2018). However, those experiments involved exposure to small-area waveguides located near the skin, and heat conduction was the dominant mode of heat transfer. Hirata et al. (2011) exposed anesthetized rats to RF energy at 1,457 MHz at whole-brain average SARs ranging from 17 to 300 W kg^{-1} and found excellent agreement between the increase in brain temperature and the BHTE using blood flow parameters measured by Doppler flowmetry. Van Leeuwen et al. (2000) found good agreement between temperature profiles in the brain subject to external cooling (by a cooling bonnet for therapeutic purposes) in a newborn infant using the bioheat equation and a detailed vascular model for the head.

MRI imaging studies provide limited additional support for the BHTE. Shrivastava et al. (2008) reported steady state temperature increases of approximately 0.2 °C in the brains of anesthetized swine exposed to RF energy at 400 MHz from a 9.4 T MRI imaging system, with a whole-head SAR of approximately 3 W kg^{-1}. Using the value for brain blood perfusion used by Morimoto et al. (2016), eqn (11b) yields a temperature increase of about 0.1 °C, which is about half of the reported value. However, that is based on the head-averaged SAR, not the local SAR at the point of measurement.

By contrast, the BHTE using fixed sets of parameters can lead to significant errors if tissue temperature is raised significantly above baseline levels. Verhaart et al. (2014) compared simulated and measured increases in brain temperature in 17 patients undergoing microwave hyperthermia treatment (434 MHz) for brain tumors. The BHTE with off-the-shelf values for the thermal parameters of head and neck tissues overpredicted the actual increase in brain temperature by 12.7 ± 11.1 °C (mean ± standard deviation) compared to an average measured temperature increase of 2 °C across all subjects. The authors attributed these differences as being due to strong thermoregulatory responses of head and neck tissues during the hyperthermia treatment.

Studies by Adair et al. (1998, 2001, 2003) provide still further support for the use of the BHTE. In those studies, the investigators exposed human subjects dorsally to RF energy at levels several times above IEEE and ICNIRP occupational limits for 45 min. The increases in skin temperature are in reasonable agreement with predictions of the two-dimensional model (Anderson et al. 2010) and three-dimensional model (Bit-Babik et al.)[5] (Table 6). (The data do not permit comparisons with temperature increases in subcutaneous tissues.) Moreover, under the conditions of Adair et al.'s experiments, the subjects experienced

Table 6. Changes in torso skin temperature in subjects exposed to extended (45 min) RF energy.

	Experimental (temperature of lower back skin for exposed subjects minus unexposed controls in different ambient temperatures)[a]					
Exposure conditions	Typical room (24 °C)	Thermally neutral environment (28 °C)	Warm environment (31 °C)	Baseline model	Multilayer model (Table 4) interpolated to the frequency	Whole-body model[b] [representative value for back, E (vertical) polarization]
100 MHz 80 W m^{-2} (Adair et al. 2003)	0.42	0.34	0.22	0.05	n.a.	0.3
450 MHz 240 W m^{-2} (Adair et al. 1998)	1.50	1.27	0.69	0.4	n.a.	1.3
2,450 MHz 350 W m^{-2} (Adair et al. 1999)	2.69	2.14	2.03	1.2	2.0	n.a.

[a]Mean of 7 subjects after 45 min exposure to dorsal surface of body. Temperatures from lower back, difference from unexposed control. From Adair et al. (1998, 1999, 2001).

[b]Bit-Babik G, Faraone A, Chou CK, Razmadze A, Zaridze R: Correlation between locally averaged SAR distribution and related temperature rise in human body exposed to RF field. BEMS 29th annual meeting, 11–15 June 2007, Kanazawa, Japan.

significant thermoregulatory responses that are not considered in the simple BHTE model used for comparison.

A final line of investigation is a study by Griffith et al. (1997), who applied heated metal probes of 1.8 and 25 cm^2 area to the skin of seven subjects at three sites (arm, leg, and torso) for extended times (2 h) while measuring the transdermal heat flux and skin temperature. For the smaller probe, the investigators found that an absorbed power density of 1 W cm^{-2} was sufficient to increase skin temperature by 68 °C over this time. Assuming that the temperature increase scales linearly with heating, this corresponds to a steady state temperature increase of 68 °C cm^2 W^{-1} and 96 °C cm^2 W^{-1} for the smaller and larger probes. The predicted increases from the BHTE (Foster et al. 2017; eqn A11) using the parameters in Table 2 are 126 and 188 °C cm^2 W^{-1} for the small and larger probes, respectively, which are twice as high as experimentally observed. This difference can be explained by a four-fold increase in skin blood flow above the baseline value at the temperatures to which the skin had been heated in the study (41–44 °C over the 2 h duration of the experiments).

In summary, the results summarized above generally support the use of the BHTE to predict the thermal response of tissue to RF exposure, although the extent of validation of the model is limited. Because the BHTE with off-the-shelf parameters does not include thermoregulatory variations in blood flow or convective cooling near thermally significant blood vessels, it is likely to yield conservative results, i.e., overestimate temperature increases. In the brain, significant thermal interactions are expected between brain tissue and cerebrospinal fluid and veins in the subarachnoid space, which some authorities consider to be a mechanism for thermal regulation of brain temperature (Wang et al. 2014). These considerations suggest that the BHTE with off-the-shelf thermal parameters will tend to overpredict the rise in tissue temperature due to exposure to RF energy, particularly if the increase above baseline temperature is more than a degree or so. However, direct experimental support for such effects, particularly in the human brain, is lacking

Comments on heating factor approach. From the studies reviewed above, the heating factor emerges as a remarkably robust quantity that relates the peak increase in temperature in tissue to the volume-averaged peak SAR. The studies reviewed above have conducted, in aggregate, thousands of different simulations for different combinations of tissue parameters and both whole-body and local exposures over a wide range of exposure conditions.

However, the overall consistency of the heating factors across the various studies may reflect, in part, the fact that all studies have used the same theoretical model (Pennes' BHTE) using similar values for the blood perfusion parameters. Most of these parameters were taken from a few tabulated summaries of data in the literature (Table 4). The thermal modeling studies need to be extended to encompass the full range of inter- and intrasubject variation, and they need to be supported by more extensive experimental data.

Comments on exposure limits. The following comments expand on those by Foster et al. (2017) and apply to thermal hazards only.

Present IEEE and ICNIRP limits are designed to protect against all established hazards of RF exposure. Above about 100 kHz, these hazards are associated with excessive heating of tissue. The documentation for both IEEE and ICNIRP limits mention 1 °C as a tolerable temperature increase.

ICNIRP: "Established biological and health effects in the frequency range from 10 MHz to a few GHz are consistent with responses to a body temperature rise of more than 1 °C."

IEEE C95.1-2005 (quoting the proceedings of a 2003 workshop; WHO 2003): "[A] 1 °C rise in temperature, even in the most sensitive tissues and organs, is not adverse" (p. 78) but is "the upper temperature increase that has no detrimental health effects."

These comments might be considered to apply to either increases in core body temperature or in local tissue temperature, which are quite different in terms of physiological significance to an individual. To increase core body temperature by 1 °C in an individual with normally functioning thermoregulation requires substantial heat input that would result in significant heat strain. For example, Adair et al. (2001) found that the core body temperature in their subjects increased by less than 0.5 °C even though the RF exposures were for extended times (45 min) at levels considerably above occupational limits. By contrast, for local exposures, a 1 °C increase in skin temperature is minor, within the range of normal variation. One can increase tissue temperature by more than 1 °C simply by taking a warm shower or drinking a cup of hot coffee.

The question arises as to what hazards the IEEE and ICNIRP limits are designed to protect against. These are discussed in detail in the rationale section of the IEEE C95.1-2005 document. Table C3 in that document lists "critical temperature levels" in various species, organs, or tissues based on experimental data. In the 2005 version of the IEEE standard, the limiting effect for setting local exposure limits was cataract formation in rabbits, which has been experimentally produced by RF exposures sufficient to increase lens temperature above 41 °C for > 30 min. Figs. 2 and 3 show that whole-body exposures compliant with present IEEE and ICNIRP reference levels will not raise local temperature of tissue to anywhere near thermally hazardous levels as summarized in the IEEE document.

An important question related to safety of handheld communications equipment is the possibility of excessive heating to the brain, which is known to be particularly sensitive to

thermal damage. Wang et al. (2014) concluded that the threshold for "progressive thermal injury [disruption to the blood-brain barrier] to the metabolically active brain cells, and the vascular endothelium appears to be between 39 and 40 °C."

Morimoto et al. (2016) found the peak temperature increase in the head at the occupational BR [10 W kg^{-1} psSAR (10 g cube)] to be about 3 °C (mean of many simulations covering frequencies between 1 and 30 GHz), ranging up to about 5 °C (Morimoto et al. 2016, Fig. 4b). The peak increase in brain temperature was about 0.8 °C (mean of many simulations) ranging up to about 1 °C (Fig. 10b in Morimoto et al. 2016). These authors defined a heating factor of the brain as the ratio of the peak temperature increase in the *brain* to the peak spatially averaged SAR in the *head*. Above about 10 GHz, the RF energy was chiefly absorbed in superficial tissues outside of the brain, while the heating factor for the brain approached a constant value of about 0.04 °C kg W^{-1}. This is a result of heat conducted into the brain from superficial tissues.

Morimoto et al. (2016) did not discuss the variation in temperature rise throughout the head. More recently that same group (Kodera et al. 2018) reported SAR and temperature profiles through cross sections of the head from RF exposures at 0.3 through 10 GHz, using a thermal model that incorporated thermoregulatory responses in the brain (from animal data). The authors found that the increase in brain temperature was localized in peripheral areas of the brain just beneath the skull. The authors concluded that the maximum local brain temperature produced by RF exposure at occupational exposure limits would be below the basal (core) brain temperature due to the fact that the periphery of the brain is 0.4–1 °C cooler than the core of the brain because of thermal interactions with the external environment (Mellergard and Nordström 1990).

These calculated temperature increases are within the range of normal physiological variability, either from the 1 °C peak-to-peak diurnal variation in brain temperature (Refinetti and Menaker 1992) or from changes in core body temperature due to exercise or taking a warm bath. The corresponding temperature increases at exposure limits for the general public will be a factor of five smaller. This work provides no basis to anticipate thermal hazards to the brain from exposures at present occupational limits, and in fact suggests that thermal consequences to the brain at such exposure levels will be minimal. The lack of direct experimental verification of the model must be acknowledged, however.

Colombi et al. (2015) have pointed to a significant inconsistency in the current exposure limits across the transition frequency: the limits above the transition are considerably more conservative against thermal hazards than those below it. The problem arises, in part, because the basic restrictions are expressed in terms of two different quantities, the psSAR below the transition and the incident power density above it.

One way to reconcile this discrepancy would be to equalize the peak temperature increase in the body above and below the transition frequency (without specifying precisely what the maximum temperature increase can be). Below the transition frequency the peak temperature increase is given by the heating factor times the local peak SAR, while above the transition frequency it can be estimated using a model such as that of Sasaki et al. (2017) in terms of incident power density on the skin. This approach makes consistent use of the same thermal model, Pennes' BHTE, with the same thermal parameters (even though the calculated temperature increases are uncertain to some extent). For this purpose, the heating factor is a useful way to generalize results of many different thermal simulations.

An alternative approach would be to specify a precise upper temperature limit and set the exposure limits accordingly. That approach is complicated, however, by the inability to calculate the thermal response of tissue with precision due to a host of potential variables (environmental, physiological, and anatomical). If, as seems to be the case, the current exposure limits below the transition frequency are sufficiently protective against thermal hazards, the former approach seems preferable. In either case, more data for the thermal response of the body to RF heating, at the modest levels that would be allowed by any reasonable set of limits, would be desirable.

CONCLUSION

Advances in computational dosimetry and thermal modeling, reviewed in this paper, have filled in many details about the relation between psSAR and peak increase in temperature. These studies show that the heating factor is a robust measure of this relation. However, additional information is needed to assess potential thermal hazards of RF exposure, including the location and magnitude of the temperature increases in the body.

This present and two previous reviews in this series (Foster et al. 2016, 2017) show that thermal models can be useful for revising and updating RF exposure limits. While the theory that underlies the models, Pennes' BHTE, is generally reliable, it is not exact. Thermal models for RF heating of tissue require additional experimental validation including effects of variability in tissue blood perfusion, possible thermoregulatory responses of the body to RF heating, and other factors. Finally, more experimental data are needed for thermal hazards of RF energy at frequencies above the threshold. Apart from thermal hazards, a comprehensive review of all reported biological effects of RF energy above the transition frequency in the standards is also needed.

Q.B., K.R.F, and M.Z. were supported in this project by Mobile and Wireless Forum, which did not review and had no control over preparation of this manuscript. The authors thank A. Hirata, Nagoya Institute of Technology, Japan, for providing results used to prepare Fig. 3, and Dr. Vitas Anderson

and Dr. C-K Chou for helpful discussion of earlier drafts of this paper. The views and opinions expressed herein are solely those of the authors and are not to be attributed to Motorola Solutions or any of its operating companies.

REFERENCES

Adair ER, Kelleher S, Mack G, Morocco T. Thermophysiological responses of human volunteers during controlled whole-body radio frequency exposure at 450 MHz. Bioelectromagnetics 19:232–245; 1998.

Adair ER, Cobb BL, Mylacraine KS, Kelleher S. Human exposure at two radio frequencies (450 and 2450 MHz): similarities and differences in physiological response. Bioelectromagnetics 20: 12–20; 1999.

Adair ER, Mylacraine KS, Cobb BL. Human exposure to 2450 MHz CW energy at levels outside the IEEE C95.1 standard does not increase core temperature. Bioelectromagnetics 22:429–439; 2001.

Adair ER, Mylacraine KS, Allen SJ. Thermophysiological consequences of whole-body resonant RF exposure (100 MHz) in human volunteers. Bioelectromagnetics 24:489–501; 2003.

Alekseev S, Radzievsky A, Szabo I, Ziskin M. Local heating of human skin by millimeter waves: effect of blood flow. Bioelectromagnetics 26:489–501; 2005.

Anderson V, Croft R, McIntosh RL. SAR versus S-inc: what is the appropriate RF exposure metric in the range 1–10 GHz? Part I: using planar body models. Bioelectromagnetics 31: 454–466; 2010.

Arkin H, Xu LX, Holmes KR. Recent developments in modeling heat transfer in blood perfused tissues. IEEE Trans Biomed Eng 41:97–107; 1994.

Baish JW. Microvascular heat transfer. In: Bronzino JB, Peterson DP, eds. Biomedical engineering handbook. 4th ed. Boca Raton, FL: CRC Press; 2014:9.1–9.16.

Bakker JF, Paulides MM, Christ A, Kuster N, van Rhoon GC. Assessment of induced SAR in children exposed to electromagnetic plane waves between 10 MHz and 5.6 GHz. Phys Med Biol 55:3115–3130; 2010.

Bakker JF, Paulides MM, Neufeld E, Christ A, Kuster N, van Rhoon GC. Children and adults exposed to electromagnetic fields at the ICNIRP reference levels: theoretical assessment of the induced peak temperature increase. Phys Med Biol 56: 4967–4989; 2011.

Colombi D, Thors B, Törnevik C. Implications of EMF exposure limits on output power levels for 5G devices above 6 GHz. IEEE Ant Wireless Prop Lett 14:1247–1249; 2015.

Foster KR, Lozano-Nieto A, Riu P. Heating of tissues by microwaves: a model analysis. Bioelectromagnetics 19:420–428; 1998.

Foster KR, Ziskin MC, Balzano Q. Thermal modeling for the next generation of radiofrequency exposure limits: commentary. Health Phys 113:41–53; 2017.

Foster KR, Ziskin MC, Balzano Q. Thermal response of human skin to microwave energy: a critical review. Health Phys 111: 528–541; 2016.

Foster-Dingley JC, van der Grond J, Moonen JEF, van den Berg-Huijsmans AA, de Ruijter W, van Buchem MA, de Craen AJM, van der Mast RC. Lower blood pressure is associated with smaller subcortical brain volumes in older persons. Am J Hypertens 28:1127–1133; 2015.

Federal Communications Commission. Evaluating compliance with FCC guidelines for human exposure to radiofrequency electromagnetic fields. FCC Bulletin OET :65; 1997.

Griffith JM, Hamilton A, Long G, Mujezinovic A, Warren D, Vij K. Human skin temperature response to absorbed thermal power. Med Imaging Ultrasonic Transducer Engin 3037: 129–134; 1997.

Hasgall PA, Di Gennaro F, Baumgartner C, Neufeld E, Gosselin MC, Payne D, Klingenböck A, Kuster N. IT'IS database for thermal and electromagnetic parameters of biological tissues [online]. 2015. Available at ***www.itis.ethz.ch/database***. Accessed 20 August 2015. DOI: 10.13099/VIP21000-03-0.

Hertzman A, Randall W. Regional differences in the basal and maximal rates of blood flow in the skin. J Appl Physiol 1: 234–241; 1948.

Hirata A, Shiozawa T. Correlation of maximum temperature increase and peak SAR in the human head due to handset antennas. IEEE Trans Microwave Theory Tech 51:1834–1841; 2003.

Hirata A, Masuda H, Kanai Y, Asai R, Fujiwara O, Arima T, Kawai H, Watanabe S, Lagroye I, Veyret B. Computational modeling of temperature elevation and thermoregulatory response in the brains of anesthetized rats locally exposed at 1. 5 GHz. Phys Med Biol 56:7639–657; 2011.

Hiura M, Nariai T, Ishii K, Sakata M, Oda K, Toyohara J, Ishiwata K. Changes in cerebral blood flow during steady state cycling exercise: a study using oxygen-15-labeled water with PET. J Cerebral Blood Flow Metabolism 34:389–396; 2014.

Institute of Electrical and Electronics Engineers. Standard for safety levels with respect to human exposure to radiofrequency electromagnetic fields, 3 kHz to 300 GHz. Piscataway, NJ: IEEE; IEEE C95.1. 2005, revised 2010.

International Commission on Non-Ionizing Radiation Protection. Guidelines for limiting exposure to time-varying electric, magnetic, and electromagnetic fields (up to 300 GHz). Health Phys 74:494–522; 1998.

International Commission on Non-Ionizing Radiation Protection. ICNIRP statement on the "guidelines for limiting exposure to time-varying electric, magnetic, and electromagnetic fields (up to 300 GHz)." Health Phys 97:257–258; 2009.

Johnson JM, Kellogg DL Jr. Local thermal control of the human cutaneous circulation. J Appl Physiol 109:1229–1238; 2010.

Kodera S, Gomez-Tames J, Hirata A. Temperature elevation in the human brain and skin with thermoregulation during exposure to RF energy. Biomed Engineering Online 17(1) [online]; 2018. Available at https://biomedical-engineering-online.biomedcentral.com/articles/10.1186/s12938-017-0432-x. Accessed 11 June 2018.

McIntosh RL, Anderson V. SAR versus S-inc: what is the appropriate RF exposure metric in the range 1–10 GHz? Part II: using complex human body models. Bioelectromagnetics 31: 467–478; 2010.

Mellergard P, Nordström C-K. Epidural temperature and possible intracerebral temperature gradients in man. Br J Neurosurg 4: 31–38; 1990.

Morimoto R, Laakso I, De Santis V, Hirata A. Relationship between peak spatial-averaged specific absorption rate and peak temperature elevation in human head in frequency range of 1–30 GHz. Phys Med Biol 61:5406–5425; 2016.

Morimoto R, Hirata A, Laakso I, Ziskin MC, Foster KR. Time constants for temperature elevation in human models exposed to dipole antennas and beams in the frequency range from 1 to 30 GHz. Phys Med Biol 62:1676–1699; 2017.

Pennes H. Analysis of tissue and arterial blood temperatures in the resting human forearm. J Appl Physiol 1:93–122; 1948.

Refinetti R, Menaker M. The circadian rhythm of body temperature. Physiol Behav 51:613–637; 1992.

Sasaki K, Mizuno M, Wake K, Watanabe S. Monte Carlo simulations of skin exposure to electromagnetic field from 10 GHz to 1 THz. Phys Med Biol 62:6993–7010; 2017.

Shrivastava D, Hanson T, Schlentz R, Gallaghar W, Snyder C, DelaBarre L, Prakash S, Iaizzo P, Vaughan JT. Radiofrequency heating at 9.4 T: in vivo temperature measurement results in swine. Magnetic Resonance Medicine 59:73–78; 2008.

Van Leeuwen G, Hand J, Lagendijk J, Azzopardi D, Edwards A. Numerical modeling of temperature distributions within the neonatal head. Pediatr Res 48:351–356; 2000.

Van Rongen E. ICNIRP exposure limits above 6 GHz, Mobile Manufacturer's Forum. Ghent, Belgium: BIOEM; 2016.

Verhaart RF, Rijnen Z, Fortunati V, Verduijn GM, van Walsum T, Veenland JF, Paulides MM. Temperature simulations in hyperthermia treatment planning of the head and neck region. Rigorous optimization of tissue properties. Strahlentherapie u Onkologie 190:1117–1124; 2014.

Walters TJ, Blick DW, Johnson LR, Adair ER, Foster KR. Heating and pain sensation produced in human skin by millimeter waves: comparison to a simple thermal model. Health Phys 78:259–267; 2000.

Wainwright PR. Computational modelling of temperature rises in the eye in the near field of radiofrequency sources at 380, 900 and 1800 MHz. Phys Med Biol 52:3335–3350; 2007.

Wang H, Wang B, Normoyle KP, Jackson K, Spitler K, Sharrock MF, Miller CM, Best C, Llano D, Du R. Brain temperature and its fundamental properties: a review for clinical neuroscientists. Front Neurosci 8:UNSP 307 [online]; 2014 Available at ***https://www.frontiersin.org/articles/10.3389/fnins.2014.00307/full***. Accessed 11 June 2018.

World Health Organization. WHO Workshop 2002: adverse temperature levels in humans. Int J Hyperther 19: 215–390; 2003.

Yeung C, Atalar E. A Green's function approach to local RF heating in interventional MRI. Med Phys 28:826–832; 2001.

Ziskin M, Alekseev S, Foster K, Balzano Q. Tissue models for RF exposure evaluation at frequencies above 6 GHz. Bioelectromagnetics 39:173–189; 2018.

■■